doi: 10.4149/gpb_2026020

KIAA1429 promotes chondrocyte senescence and ferroptosis in osteoarthritis progression by facilitating m6A-mediated downregulation of USP3

Binqing Ma[1], Jiangbo Zhao[1], Chen Cheng[1] and Biao Yang[1]

[1] *Department of Joint Surgery and Sports Medicine, Hospital of Shaanxi Nuclear Industry, Xianyang, China*

Abstract. Osteoarthritis (OA) is a common orthopedic disorder with complicated pathological mechanisms. This study aimed to uncover a novel regulatory network related to vir-like m6A methyltransferase-associated protein KIAA1429 (also known as VIRMA) and ubiquitin-specific protease 3 (USP3) in the progression of OA. An *in vitro* model of OA was constructed by treating chondrocytes (C28/I2) with interleukin-1β (IL-1β). qRT-PCR and Western blot were applied for gene and protein expression detection. Cell viability was examined using a CCK-8 assay. Cell death was evaluated by flow cytometry following Annexin V/PI staining. Cell senescence was assessed by senescence-associated β-galactosidase (SA-β-gal) staining. Ferroptosis-related events were detected by commercial kits. The interaction between KIAA1429 and USP3 was confirmed *via* RNA immunoprecipitation assay and dual-luciferase reporter assay. OA mice model was induced by surgical destabilization of the medial meniscus (DMM). Results showed that KIAA1429 expression was up-regulated in C28/I2 cells after IL-1β exposure. Inhibition of KIAA1429 impeded senescence and ferroptosis in IL-1β-treated C28/I2 cells. Mechanistically, KIAA1429 reduced USP3 mRNA expression through m6A methylation modification. Moreover, the protective effects of KIAA1429 knockdown on IL-1β-induced senescence and ferroptosis in C28/I2 cells were rescued by USP3 downregulation. *In vivo,* KIAA1429 downregulation suppressed the development of OA in DMM mice. These results elucidate that KIAA1429 promotes the senescence and ferroptosis of chondrocytes by increasing m6A methylation of USP3 to suppress its stability, thereby contributing to the pathogenesis of OA.

Key words: Osteoarthritis — KIAA1429 — USP3 — m6A modification — Senescence — Ferroptosis

Introduction

Osteoarthritis (OA) is a degenerative joint disease with a significantly rising incidence and prevalence (Mandl 2019). OA is accompanied by the pathogenic manifestations including destruction and loss of articular cartilage, further resulting in joint pain and dysfunction (Yao et al. 2023; Hongyao et al. 2024). Chondrocytes in articular cartilage have an essential function in regulating cartilage homeostasis (Fujii et al. 2022). Cellular senescence is considered to play a pivotal role in cartilage degradation and OA pathology (Coryell et al. 2021). OA chondrocytes exhibit characteristics of cellular senescence, such as telomere shortening and increased senescence-associated β-galactosidase (SA-β-gal) activity (Rim et al. 2020). In addition, ferroptosis of normal chondrocytes can accelerate the progression of OA and discovering the ferroptosis-related regulators may contribute to the treatment of OA (Liu D et al. 2024). Despite these insights, the molecular crosstalk between senescence and ferroptosis in chondrocytes remains poorly understood.

Correspondence to: Biao Yang, Department of Joint Surgery and Sports Medicine, No. 215 Hospital of Shaanxi Nuclear Industry, No. 35 Weiyang West Road, Qindu District, Xianyang 712000, China
E-mail: yb1572250988@163.com

© The Authors 2026. This is an **open access** article under the terms of the Creative Commons Attribution-NonCommercial 4.0 International License (https://creativecommons.org/licenses/by-nc/4.0/), which permits non-commercial use, distribution, and reproduction in any medium, provided the original work is properly cited.

N6-methyladenosine (m6A) is one of the most prevalent RNA modifications, with important regulation in the onset and progression of OA (Radbakhsh et al. 2025; Yu et al. 2025). Vir-like m6A methyltransferase-associated protein (KIAA1429, also known as VIRMA) is another key component of the m6A methyltransferase complex, playing vital biological and pharmacological roles in human diseases (Zhang et al. 2022). A recent study has indicated that KIAA1429 facilitates chondrocyte ferroptosis in OA (Liu Y et al. 2024). KIAA1429 also hindered collagen synthesis and alleviated ultraviolet ray (UVR)-induced photoaging *via* mediating m6A modification of MFAP4 (Liu Y et al. 2024). In H_2O_2-induced premature senescence of human embryonic lung fibroblasts, KIAA1429 was down-regulated with potential as an epigenetic biomarker to cell senescence and associated diseases (Wu et al. 2022). However, the effect of KIAA1429 on chondrocyte senescence in OA remains unclear. Ubiquitin-specific protease 3 (USP3) belongs to deubiquitinases (DUBs) that can counteract ubiquitination to maintain homeostasis (Wang et al. 2024). The recent study suggested the protective function of USP3 against IL-1β-induced chondrocyte apoptosis in OA (Zhou et al. 2019). USP3 mRNA has been predicted to contain an m6A site; however, the association between KIAA1429 and USP3 remains unexplored.

This study investigated the hypothesized interaction between KIAA1429 and USP3, mediated by m6A methylation. The primary aim was to elucidate the roles of KIAA1429 and USP3 in chondrocyte senescence and ferroptosis during OA progression, and to identify potential therapeutic targets for OA.

Materials and Methods

Database analysis

Down-regulated and up-regulated genes in cartilage tissues from OA patients were predicted by the GSE51588 dataset (https://www.ncbi.nlm.nih.gov/geo/query/acc.cgi?acc = GSE51588).

Table 1. Primer sequences used for qPCR

		Primers for qPCR (5'–3')
KIAA1429	F:	AAGTGCCCCTGTTTTCGATAG
	R:	ACCAGACCATCAGTATTCACCT
USP3	F:	ATGAATGCCATCCTTCAGTCAC
	R:	GGTGTGGTATGTCCGCCTT
GAPDH	F:	CAAATTCCATGGCACCGTCA
	R:	GACTCCACGACGTACTCAGC

F, forward; R, reverse.

IL-1β induction and cell transfection

Human chondrocyte cell line C28/I2 (BioVector NTCC Inc., Beijing, China) was cultured in a temperature incubator at 37°C with 5% CO_2. The complete medium for C28/I2 consisted of DMEM, 10% fetal bovine serum, and 1% penicillin-streptomycin solution. These reagents were derived from Gibco (Carlsbad, CA, USA). To construct a cell model of OA, C28/I2 cells were treated with IL-1β (Sigma, St. Louis, MO, USA) at concentrations of 5 ng/ml, 10 ng/ml, or 20 ng/ml for 24 h.

Small interfering (si) RNAs targeting KIAA1429 (siKIAA1429) or USP3 (siUSP3), and the non-targeting siRNA (siNC) were provided by RIBOBIO (Guangzhou, China). In strict accordance with the manufacturer's specification, transfection procedures in C28/I2 cells were performed by Lipofectamine™ 3000 Kit (Invitrogen, Carlsbad, CA, USA). For cell transfection involving IL-1β treatment, the cells were transfected after IL-1β treatment.

Real-time quantitative polymerase chain reaction (RT-qPCR)

QIAzol Lysis Reagent (Qiagen, Hilden, Germany) was utilized for total RNA extraction from cells or tissues. Reverse transcription was carried out through QuantiTect Reverse Transcription Kit (Qiagen). Then, qPCR was performed by SYBR Green Realtime PCR Master Mix (Toyobo, Osaka, Japan) using the obtained cDNA and the synthesized primers (Table 1). KIAA1429 and USP3 levels were analyzed *via* the $2^{-\Delta\Delta Ct}$ method, with GAPDH serving as the internal control.

Western blot

C28/I2 cells were collected and lysed with RIPA buffer (Sigma), and then an equal amount of proteins (50 μg) was isolated through gel electrophoresis. After proteins were transferred to PVDF membranes (Sigma), blocking buffer (Beyotime, Shanghai, China) was used to prevent non-specific protein binding. The primary antibodies were incubated overnight at 4°C and the secondary antibody was incubated for 1 h at room temperature. After detection using the ECL Kit (Beyotime), protein signals were analyzed using ImageJ software. All antibodies were listed as below: anti-KIAA1429 (Proteintech, Wuhan, China; 30166-1-AP), anti-USP3 (Proteintech, 12490-1-AP), anti-p16 (Proteintech, 30519-1-AP), anti-p21 (Proteintech, 10355-1-AP), anti-SLC7A11 (Proteintech, 26864-1-AP), anti-ACSL4 (Proteintech, 22401-1-AP), anti-GAPDH (Abcam, Cambridge, UK; ab9485), and Goat Anti-Rabbit IgG H&L (HRP) (Abcam, ab205718).

Cell counting kit-8 (CCK-8) assay

C28/I2 cells were inoculated into 96-well plates, cultured overnight, and then subjected to IL-1β treatment or transfec-

tion for 48 h. CCK-8 solution (Sigma) was added to culture plates, followed by the examination of the optical density (OD) value at 450 nm *via* a microplate reader.

Flow cytometry

C28/I2 cells were stained with Annexin V-FITC and propidium iodide (PI) following the instruction of Annexin V-FITC Apoptosis Detection Kit (Sigma). Flow cytometric analysis was promptly carried out using a FACScan instrument (BD Biosciences, San Diego, CA, USA). Dead cells were defined as the summation of late apoptotic cells (Annexin V^+/PI^+) and necrotic cells (Annexin V^-/PI^+).

SA-β-gal assay

C28/I2 cells were stained using a Senescence β-gal Staining Kit (Beyotime). Cells were washed with phosphate buffer solution (PBS; Gibco) and fixed with staining fixative solution at room temperature for 15 min. Then, the cells were incubated with staining working solution at 37°C overnight. Positive (blue) cells were counted in five randomly selected fields of view at 100× magnification.

Ferroptosis-related events

Reactive oxygen species (ROS) level was measured *via* ROS Assay Kit (Beyotime) through a flow cytometer. Glutathione (GSH) level detection was conducted using the GSH Assay Kit (Beyotime) and quantified by a microplate reader. The operation steps were in accordance with the supplied manuals. Fe^{2+} level was examined by an Iron assay kit (Sigma) as required by the manufacturer. Briefly, cells were treated with an iron reducer to convert Fe^{3+} to Fe^{2+}, followed by incubation with an iron probe and measurement of the absorbance.

RNA immunoprecipitation (RIP) assay

For m6A-RIP, the m6A methylation RIP Kit (RIBOBIO) was used in accordance with the instructions. Briefly, total RNA from C28/I2 cells was fragmented and incubated with protein A/G magnetic beads conjugated with anti-m6A or anti-IgG. Then the bound RNA was eluted and m6A-modified USP3 mRNA was detected using qPCR. For KIAA1429-RIP, Imprint® RNA Immunoprecipitation Kit (Sigma) was applied according to the user's guidance. Lysates of C28/I2 cells were incubated with protein A/G magnetic beads pre-coated with anti-KIAA1429 or anti-IgG at 4°C overnight. The beads were washed with PBS and treated with proteinase K for 30 min. Then complexes were collected and RNA was purified for qPCR detection of USP3.

USP3 mRNA stability

USP3 mRNA stability was assessed by treatment with actinomycin D. C28/I2 cells were incubated with 2 μg/ml actinomycin D (Sigma). These cells were harvested at continuous time points (0 h, 4 h, 8 h, and 12 h), and then USP3 mRNA expression was quantified using qPCR.

Dual-luciferase reporter assay

The SRAMP database (http://www.cuilab.cn/sramp) was used to predict the m6A site in USP3 mRNA. USP3 sequence containing m6A site (474) and its sequence containing the mutated m6A site were inserted into the pGL4 vector (Promega, Beijing, China), respectively. The obtained wild-type USP3 (WT-USP3) or mutant-type USP3 (MUT-USP3) was co-transfected into C28/I2 cells with siNC or siKIAA1429. Dual-luciferase Reporter Assay System (Promega) was utilized for the examination of relative luciferase activity.

Animal assay

An OA model was established in 8-week-old C57BL/6 mice (SPF Biotech, Beijing, China) by performing Destabilization of the Medial Meniscus (DMM) surgery, as previously described (Glasson et al. 2007). Adeno-associated virus (AAV) is a gene therapy vector enabling long-term protein expression, and commonly used in OA animal research (Zhou et al. 2025). AAV vector elicits almost no host immune response suitable for long-term *in vivo* research including chronic disease model, compared to other models such as adenovirus (high inflammatory response), lentivirus (potential insertion mutation), or non-viral plasmid transfection (ephemeral expression efficiency). The mice in the sham group suffered from the excision of the skin of the right knee joint without damaging the ligaments. After DMM operation for one week, AAV-packaged shKIAA1429 (5 μl, 1×10^9 PFU) or AAV alone was injected into the knee joint once a week. There were 6 mice in each group (the sham, the DMM+AAV, or the DMM+AAV-shKIAA1429 group). After the third injection, mice were euthanized and knee tissues were collected for histological analysis (HE staining and Safranin O staining). In addition, cartilage tissues were homogenized for ferroptosis detection (ROS, GSH, and Fe^{2+}) and Western blot analysis. Ethical approval for the study was acquired from the Animal Care Committee of No. 215 Hospital of Shaanxi Nuclear Industry. Guide for the Care and Use of Laboratory Animals was strictly followed in the present study. The name of the guidelines followed for the welfare of the laboratory animals: The National Institutes of Health guide for the care and use of Laboratory animals (NIH Publications No. 8023, revised 1978).

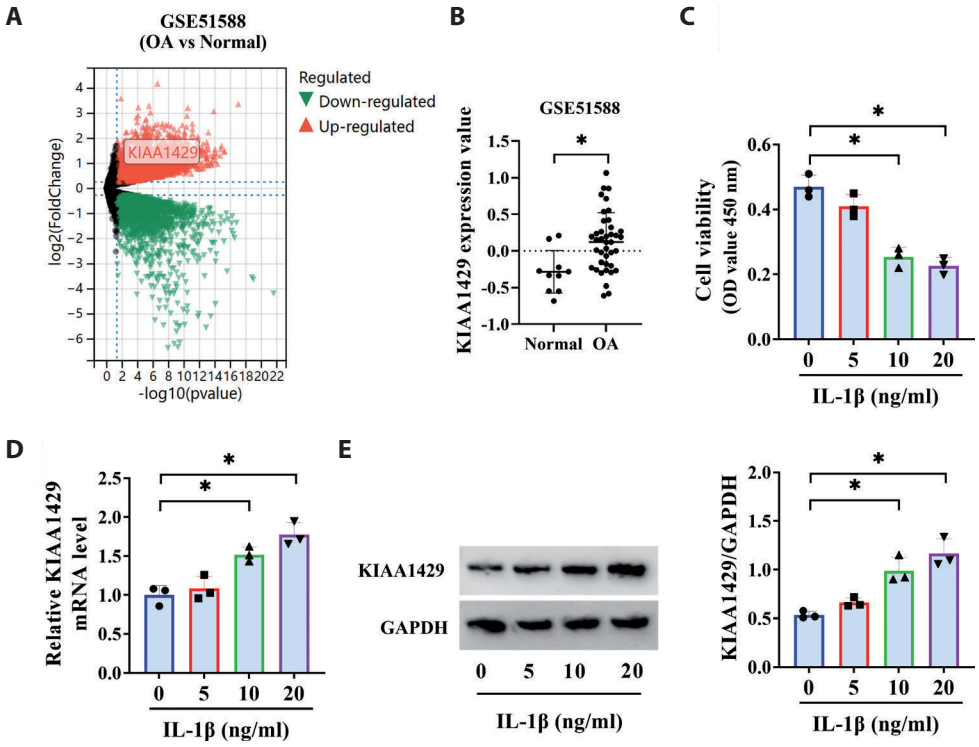

Figure 1. IL-1β induced the upregulation of KIAA1429 in C28/I2 cells. **A.** Volcano plot of dysregulated gene including KIAA1429 (up-regulated) in OA from GSE51588 dataset. Red, up-regulated; green, down-regulated. **B.** KIAA1429 expression in cartilage tissues of OA patients ($n = 40$) and normal controls ($n = 10$) in GSE51588 dataset. **C.** Cell viability was examined using CCK-8 assay after C28/I2 cells were treated with IL-1β of 0 ng/ml, 5 ng/ml, 10 ng/ml, or 20 ng/ml. KIAA1429 mRNA (**D**) and protein (**E**) detection was performed by qPCR and Western blot in C28/I2 cells with IL-1β treatment of 0 ng/ml, 5 ng/ml, 10 ng/ml, or 20 ng/ml. * $p < 0.05$.

Statistical analysis

Linear relation between KIAA1429 and USP3 was analyzed using Pearson's correlation coefficient. Distribution normality was evaluated using Shapiro-Wilk normality test. The homogeneity of variance was tested by Levene test. Data were obtained from three independent assays, and then revealed as mean ± SD. SPSS was utilized for data analysis, and $p < 0.05$ represented the significant difference after analysis by Student's *t*-test (for two groups) or ANOVA followed by Tukey's test (multiple groups).

Results

IL-1β induced KIAA1429 upregulation in C28/I2 cells

To analyze the expression change of KIAA1429 in OA, researchers focused on the online GEO database (GSE51588 dataset). Analysis revealed dysregulated genes in the cartilage tissues of OA patients, with KIAA1429 being significantly upregulated (Fig. 1A). The expression value of KIAA1429 in OA samples ($n = 40$) from the GSE51588 dataset is shown in Figure 1B. To model OA *in vitro*, C28/I2 cells were stimulated with IL-1β. CCK-8 detection manifested that cell viability was prominently reduced by IL-1β (10 ng/ml or 20 ng/ml) (Fig. 1C). The effect of IL-1β on KIAA1429 expression was analyzed using qPCR and Western blot. As indicated in Figure 1D and E, KIAA1429 expression at the mRNA and protein levels was evidently increased in the 10 ng/ml and 20 ng/ml IL-1β groups relative to the 0 ng/ml group. For subsequent experiments, a concentration of 10 ng/ml IL-1β was used for treatment. These data demonstrate that abnormal upregulation of KIAA1429 implies its potential role in OA.

KIAA1429 knockdown attenuated cell senescence in IL-1β-induced C28/I2 cells

KIAA1429 knockdown was achieved by siKIAA1429 transfection for the functional analysis of KIAA1429 in OA. According to the results of Western blot, KIAA1429 protein expression was significantly downregulated after transfection with siKIAA1429 (Fig. 2A). IL-1β-induced

KIAA1429 protein upregulation was reversely inhibited by siKIAA1429 (Fig. 2B). Cell viability was enhanced in the IL-1β+siKIAA1429 group in comparison with the IL-1β+siNC group (Fig. 2C). Flow cytometry showed that IL-1β accelerated cell death, whereas KIAA1429 knockdown attenuated IL-1β-induced this effect (Fig. 2D). In the SA-β-gal assay,

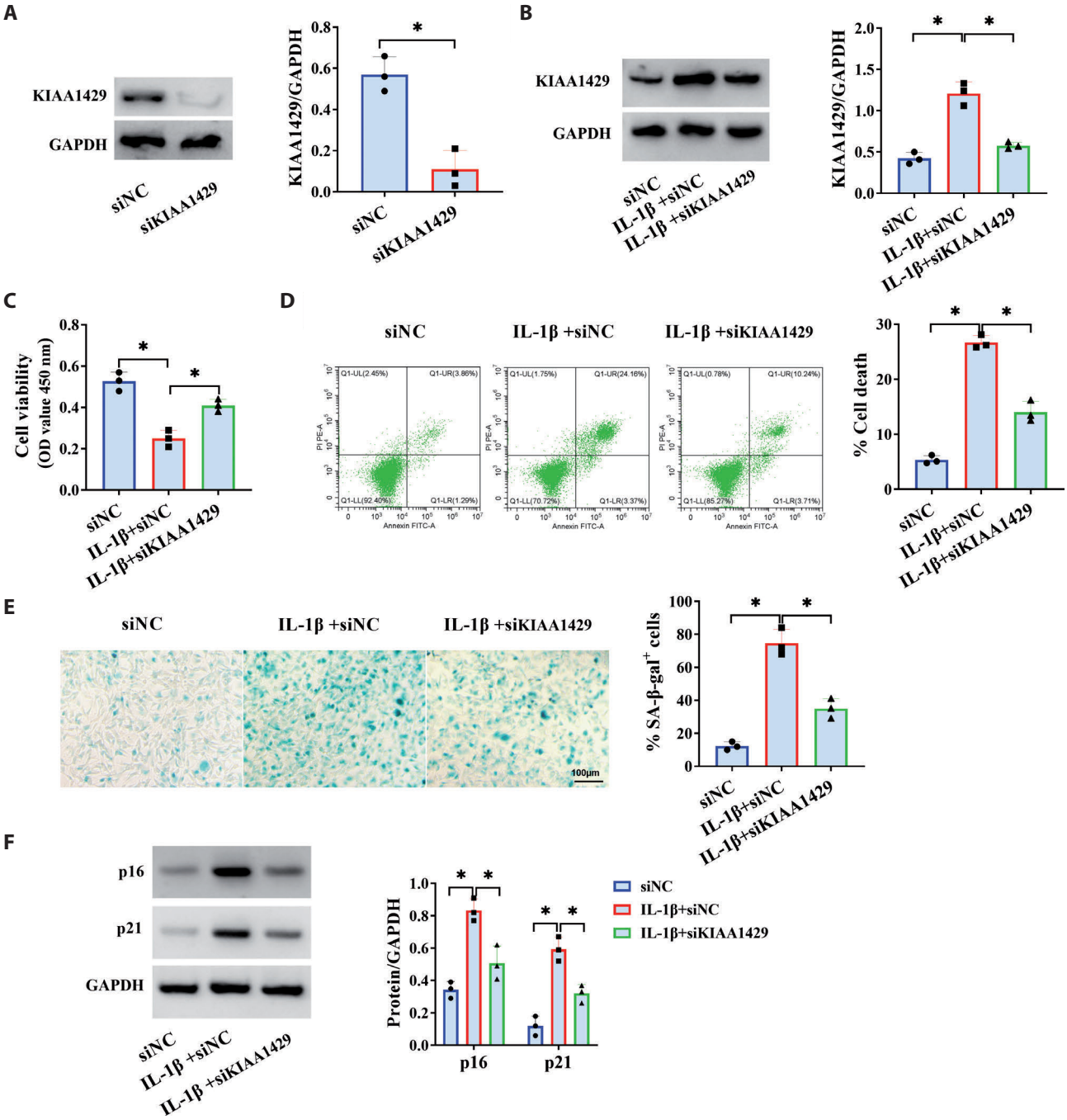

Figure 2. KIAA1429 knockdown attenuated cell senescence in IL-1β-induced C28/I2 cells. **A.** C28/I2 cells were transfected with siNC or siKIAA1429, and then transfection efficiency of siKIAA1429 was assessed by Western blot with GAPDH as the internal control. B–F. C28/I2 cells were treated with siNC, 10 ng/ml IL-1β+siNC, or IL-1β+siKIAA1429. **B.** Western blot was conducted for protein analysis of KIAA1429, with GAPDH as the internal control. **C.** CCK-8 was used for examination of cell viability (OD value at 450 nm). **D.** Flow cytometry was applied to determine cell death rate. **E.** SA-β-gal staining was utilized to measure SA-β-gal$^+$ cells to assess cell senescence. Scale bar = 100 μm. **F.** Western blot was used to detect the protein levels of senescence-related markers p16 and p21, with GAPDH as the internal control. * $p < 0.05$.

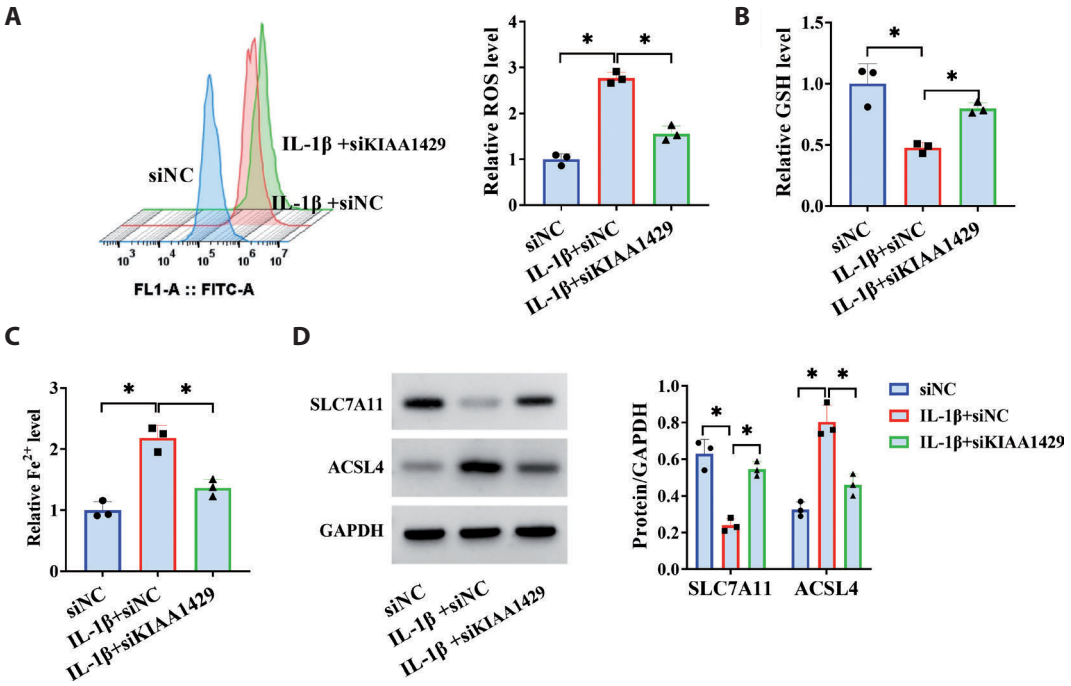

Figure 3. KIAA1429 knockdown suppressed IL-1β-mediated ferroptosis in C28/I2 cells. C28/I2 cells were divided into siNC, 10 ng/ml IL-1β+siNC, and IL-1β+siKIAA1429 groups. **A.** Flow cytometry was performed to detect ROS level. **B.** GSH level of each group. **C.** Fe^{2+} level was detected by iron assay kit. **D.** Ferroptosis-associated markers SLC7A11 and ACSL4 were examined by Western blot, with GAPDH as the internal control. * $p < 0.05$.

siKIAA1429 treatment reduced SA-β-gal positive cells upon IL-1β treatment, which testified that IL-1β-induced cell senescence was blocked following knockdown of KIAA1429 (Fig. 2E). The proteins associated with cell senescence were determined using Western blot. IL-1β treatment largely elevated the protein levels of p16 and p21, but these changes were abolished with the knockdown of KIAA1429 (Fig. 2F). Thus, IL-1β-induced cell senescence was prevented by KIAA1429 knockdown in C28/I2 cells.

KIAA1429 knockdown suppressed IL-1β-mediated ferroptosis in C28/I2 cells

To assess the regulation of KIAA1429 in ferroptosis, a series of detections were performed after IL-1β induction and siKIAA1429 transfection. IL-1β treatment resulted in increases of ROS (Fig. 3A) and decreases of GSH levels (Fig. 3B), whereas these events were obviously ameliorated when KIAA1429 was knocked down. Meanwhile, C28/I2 cells in the IL-1β+siKIAA1429 group exhibited an inhibitory effect on Fe^{2+} level, relative to IL-1β-treated C28/I2 cells without KIAA1429 knockdown (Fig. 3C). In Western blot analysis, SLC7A11 downregulation and ACSL4 upregulation triggered by IL-1β were distinctly restored by downregulation of KIAA1429 (Fig. 3D). Thus, silencing KIAA1429 repressed ferroptosis in IL-1β-induced C28/I2 cells.

KIAA1429 inhibited USP3 mRNA in an m6A-dependent manner

Analysis of the GSE51588 dataset identified USP3 as a significantly down-regulated gene in OA cartilage tissues (Fig. 4A,B). Pearson's correlation coefficient analysis showed a negative correlation between KIAA1429 and USP3 expression in OA samples from the GSE51588 dataset (Fig. 4C). Then, the results showed that both the mRNA and protein levels of USP3 were lower in the 10 ng/ml and 20 ng/ml IL-1β groups than those in the 0 ng/ml IL-1β group (Fig. 4D,E). Furthermore, siKIAA1429 transfection counteracted IL-1β-induced inhibition of the mRNA and protein of USP3 (Fig. 4F,G). The RIP assay demonstrated that KIAA1429 knockdown reduced m6A-modified USP3 mRNA levels in IL-1β-induced C28/I2 cells (Fig. 4H). Additionally, KIAA1429-RIP results showed that the interaction between KIAA1429 protein and USP3 mRNA was decreased after knockdown of KIAA1429 in IL-1β-induced C28/I2 cells (Fig. 4I). After actinomycin D treatment, KIAA1429 inhibition enhanced USP3 mRNA stability in IL-1β-treated C28/I2 cells (Fig. 4J).

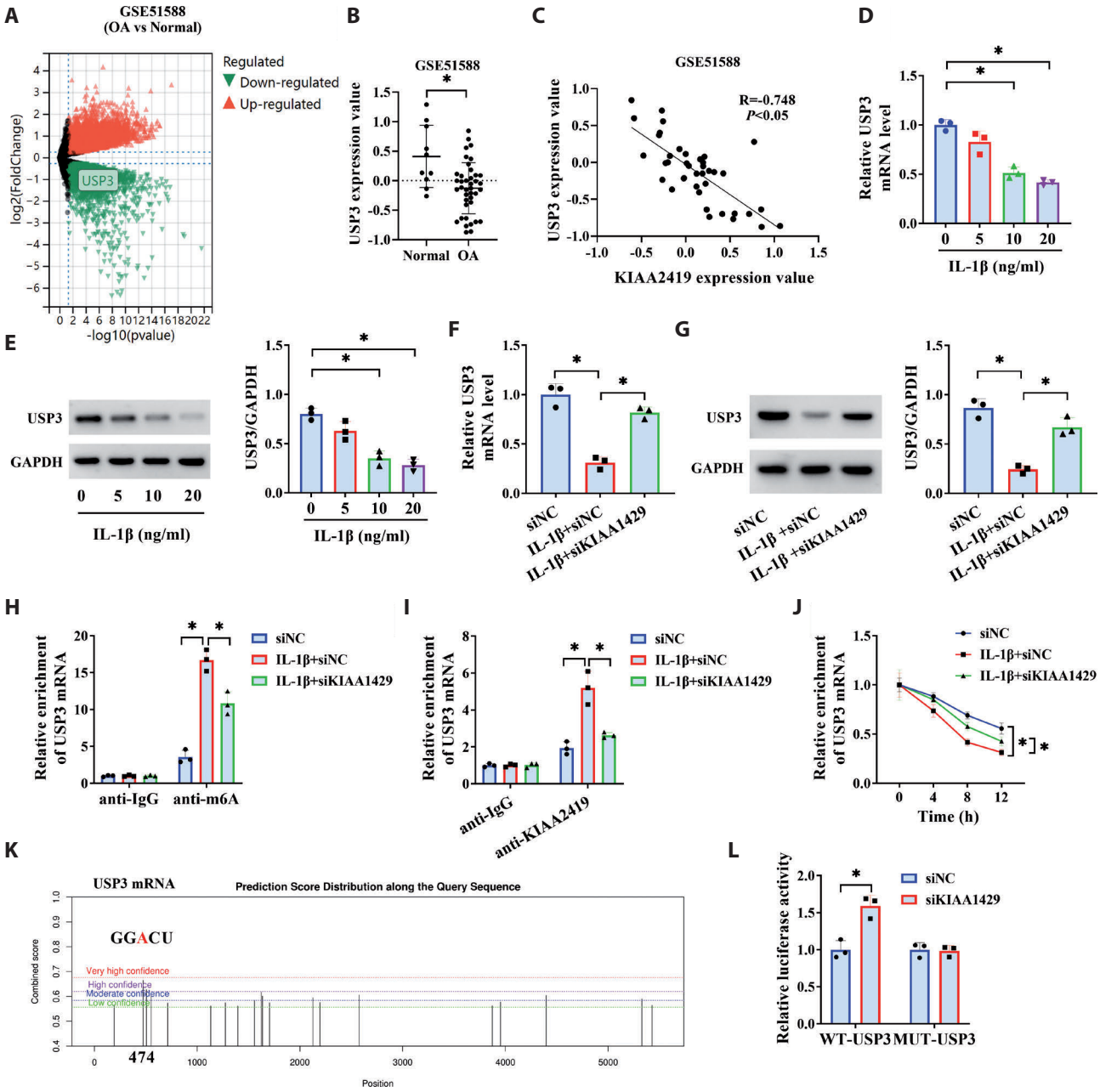

Figure 4. KIAA1429 inhibited USP3 mRNA in an m6A-dependent manner. **A.** Volcano plot from GSE51588 dataset showed the dysregulated gene including USP3 (down-regulated) in OA. Red, up-regulated; green, down-regulated. **B.** USP3 expression analysis in OA cartilage tissues ($n = 40$) relative to normal controls ($n = 10$) according to the GSE51588 dataset. **C.** Linear analysis between KIAA1429 and USP3 expression was carried out using Pearson's correlation coefficient. **E.** USP3 mRNA analysis was conducted through qPCR. **D.** Protein detection was conducted using Western blot (**E**) after exposure to IL-1β (0 ng/ml, 5 ng/ml, 10 ng/ml, or 20 ng/ml). USP3 mRNA (**F**) and protein (**G**) levels were measured by qPCR and Western blot in the si-NC group, the 10 ng/ml IL-1β+siNC group, and the IL-1β+siKIAA1429 group, with GAPDH as the internal control. **H.** The m6A modification between KIAA1429 and USP3 was verified *via* m6A-RIP. Total RNA from C28/I2 cells (in the siNC group, the 10 ng/ml IL-1β+siNC group, or the IL-1β+siKIAA1429 group) was fragmented and incubated with anti-IgG or anti-m6A coated with magnetic beads, then USP3 mRNA enrichment was detected. **I.** Interaction between KIAA1429 and USP3 was confirmed using KIAA1429-RIP. USP3 mRNA enrichment was examined after lysing C28/I2 cells (in the siNC group, the 10 ng/ml IL-1β+siNC group, or the IL-1β+siKIAA1429 group) were precipitated with anti-IgG or anti-KIAA1429 coated magnetic beads. **J.** USP3 mRNA stability was assessed through qPCR in IL-1β-treated C28/I2 cells after siKIAA1429 transfection and actinomycin D treatment for 0 h, 4 h, 8 h, or 12 h in IL-1β-treated C28/I2 cells. **K.** SRAMP database was used to predict m6A sites in USP3 mRNA. **L.** Dual-luciferase reporter assay was performed to validate m6A site between KIAA1429 and USP3. * $p < 0.05$.

SRAMP showed that position 474 is an m6A modification site in USP3 mRNA with the highest prediction score (Fig. 4K). Moreover, the dual-luciferase reporter assay indicated that the relative luciferase activity of WT-USP3 was significantly increased after KIAA1429 knockdown, but the luciferase activity of MUT-USP3 was not affected

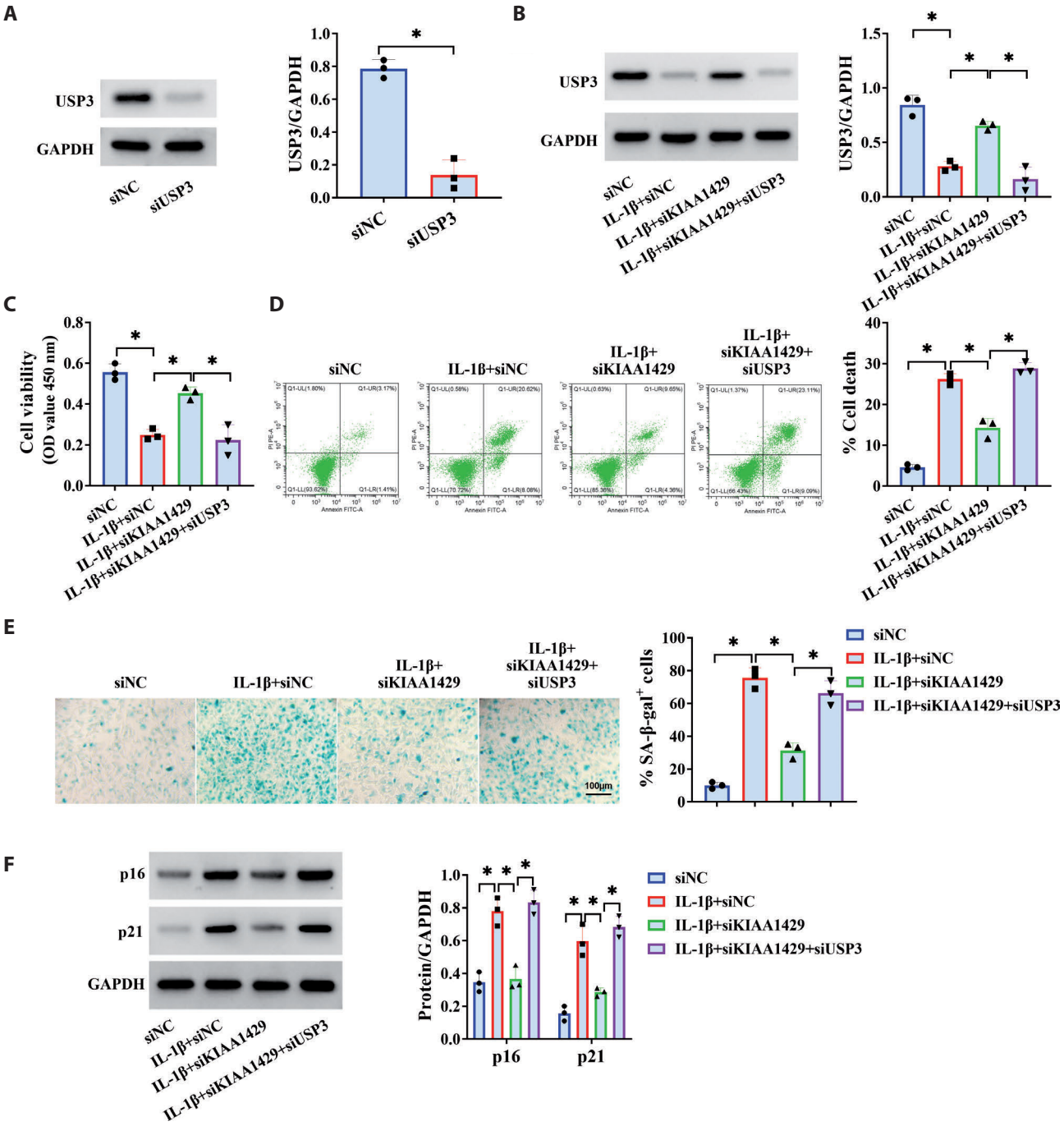

Figure 5. KIAA1429/USP3 axis regulated IL-1β-induced cell senescence in C28/I2 cells. **A.** Knockdown effect of siUSP3 (compared to siNC) was assessed using Western blot, with GAPDH as the internal control. B–F. C28/I2 cells were divided into the siNC group, the 10 ng/ml IL-1β+siNC group, the IL-1β+siKIAA1429 group, or the IL-1β+siKIAA1429+siUSP3 group. **B.** USP3 protein examination was conducted by Western blot, with GAPDH as the internal control. **C.** Cell viability detection (OD value of 450 nm) was conducted using CCK-8 assay. **D.** Cell death analysis was conducted by flow cytometry. **E.** Cell senescence assessment was performed through SA-β-gal staining. Scale bar = 100 μm. **F.** The protein detection of senescence-related markers p16 and p21 was performed by Western blot, with GAPDH as the internal control. * $p < 0.05$.

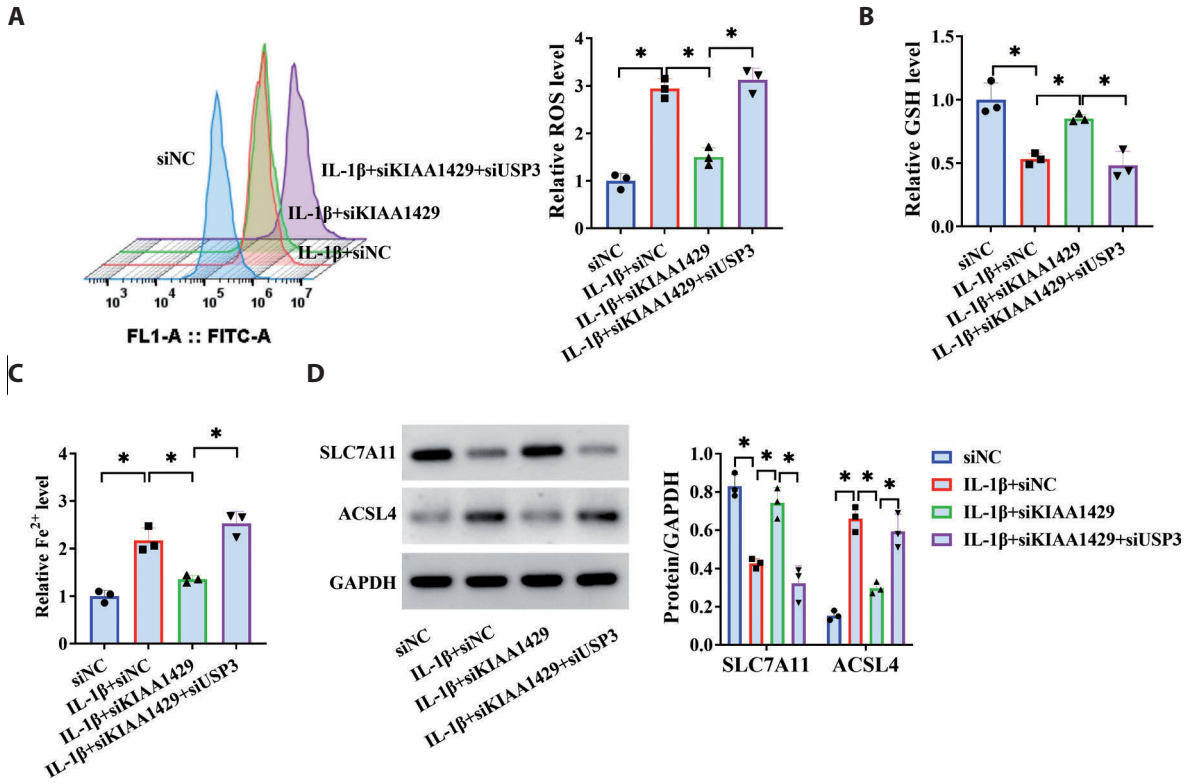

Figure 6. KIAA1429 silence abated IL-1β-induced ferroptosis *via* upregulating USP3 in C28/I2 cells. C28/I2 cells were divided into the siNC group, the 10 ng/ml IL-1β+siNC group, the IL-1β+siKIAA1429 group, and the IL-1β+siKIAA1429+siUSP3 group. **A.** ROS level analysis by flow cytometric method **B.** GSH level analysis by a commercial kit. **C.** Fe^{2+} level detection *via* iron assay kit. **D.** Expression analysis of ferroptosis-associated markers SLC7A11 and ACSL4 through Western blot, with GAPDH as the internal control. * $p < 0.05$.

by KIAA1429 silencing (Fig. 4L). Thus, KIAA1429 acted as an m6A scaffolding protein to affect USP3 mRNA in the OA cell model.

KIAA1429/USP3 axis regulated IL-1β-induced cell senescence in C28/I2 cells and primary human chondrocytes

Interaction between KIAA1429 and USP3 in regulating IL-1β-induced cell senescence was further explored using C28/I2 cells. Firstly, USP3 was knocked down after siUSP3 transfection according to Western blot results (Fig. 5A). After IL-1β treatment, siKIAA1429-induced upregulation of USP3 was hindered by siUSP3 (Fig. 5B). KIAA1429 knockdown-induced promoting effect on cell viability (Fig. 5C) and the suppressive effect on cell death (Fig. 5D) were attenuated following USP3 downregulation in IL-1β-treated chondrocytes. In addition, knockdown of both KIAA1429 and USP3 increased SA-β-gal positive cells relative to KIAA1429 knockdown alone after IL-1β stimulation (Fig. 5E). Likewise, the inhibition of p16 and p21 protein expression triggered by siKIAA1429 in IL-1β-treated C28/I2 cells was reversed when USP3 was down-regulated (Fig. 5F). Thus, cell senescence induced by IL-1β was relieved by KIAA1429 knockdown by increasing USP3 expression.

KIAA1429 silence abated IL-1β-induced ferroptosis by upregulating USP3 in C28/I2 cells

The study continued to analyze the regulation of KIAA1429 and USP3 in IL-1β-induced ferroptosis. After siUSP3 transfection into IL-1β-treated C28/I2 cells, siKIAA1429-mediated ROS level reduction (Fig. 6A) and GSH level increase (Fig. 6B) were observed with significant changes. Fe^{2+} level was elevated after co-transfection with siKIAA1429 and siUSP3 in IL-1β-stimulated C28/I2 cells, in contrast to alone siKIAA1429 transfection (Fig. 6C). Through Western blot detection, SLC7A11 upregulation and ACSL4 downregulation caused by KIAA1429 inhibition were also found to be restored after knockdown of USP3 under the treatment of IL-1β (Fig. 6D). All in all, KIAA1429 silence up-regulated USP3 to inhibit ferroptosis in IL-1β-treated C28/I2 cells.

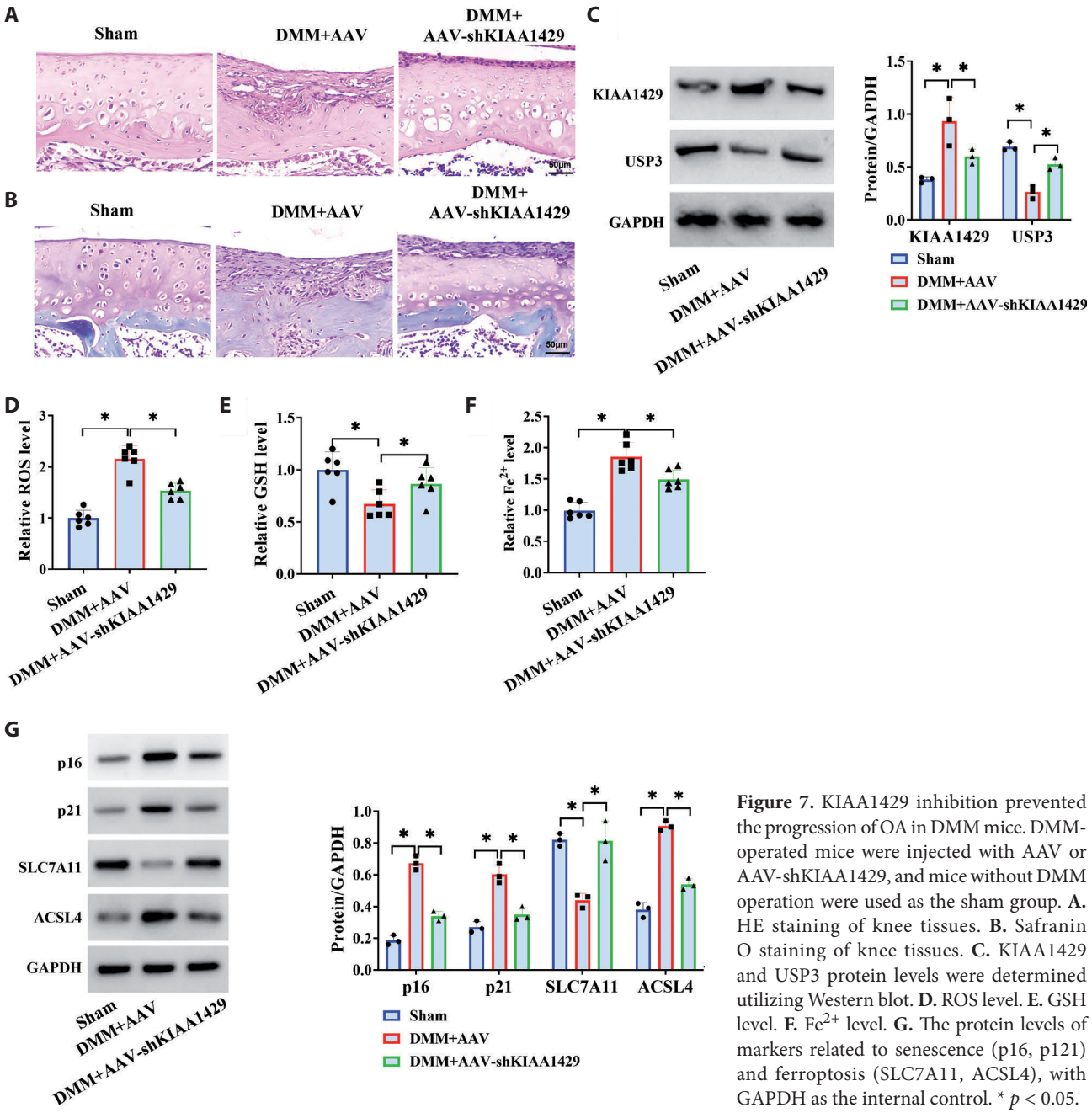

Figure 7. KIAA1429 inhibition prevented the progression of OA in DMM mice. DMM-operated mice were injected with AAV or AAV-shKIAA1429, and mice without DMM operation were used as the sham group. **A.** HE staining of knee tissues. **B.** Safranin O staining of knee tissues. **C.** KIAA1429 and USP3 protein levels were determined utilizing Western blot. **D.** ROS level. **E.** GSH level. **F.** Fe^{2+} level. **G.** The protein levels of markers related to senescence (p16, p121) and ferroptosis (SLC7A11, ACSL4), with GAPDH as the internal control. * $p < 0.05$.

KIAA1429 inhibition prevented the progression of OA in DMM mice

OA was induced in mice *via* destabilization of the DMM surgery, and histological analysis was performed using the collected knee tissues. The HE staining suggested that chondrocyte arrangement in the articular cartilage of DMM mice was disordered, whereas the effect was partially mitigated by KIAA1429 knockdown (Fig. 7A). Safranin O staining revealed severe cartilage damage, which was significantly improved by KIAA1429 downregulation (Fig. 7B). Western blot indicated the increased expression of KIAA1429 and reduced expression of USP3 in DMM mice, but these effects were attenuated after injection with AAV-shKIAA1429 (Fig. 7C). Cartilage from DMM mice exhibited increased ROS and Fe^{2+} levels, along with decreased GSH levels; however, knockdown of KIAA1429 significantly mitigated these ferroptosis-related changes (Fig. 7D–F). The protein levels

of p16, p21, and ACSL4 were up-regulated but SLC7A11 was down-regulated in DMM+AAV group, which was overturned by remarkable changes following KIAA1429 silence (Fig. 7G,H). Taken together, these findings indicate that KIAA1429 downregulation suppresses the progression of OA in DMM mice.

Discussion

IL-1β has been reported to act as a critical mediator in the initiation and progression of OA (Liu et al. 2023). OA is primarily driven by inflammatory responses that are now recognized as central to OA pathophysiology (Knights et al. 2023). In OA joints, pro-inflammatory cytokines such as IL-1β are markedly upregulated and contribute to ROS production (Wan et al. 2023). In line with these findings, the study employed IL-1β to simulate OA-like conditions in chondrocytes *in vitro*. The observed reduction in cell viability and acceleration of cellular senescence confirmed the successful induction of an OA model, consistent with established methodologies.

Among various post-transcriptional regulators, RNA modifications – especially m6A – have garnered increasing attention for their roles in numerous biological processes (Wen et al. 2024; Ren et al. 2025). Multiple m6A regulators have been implicated in OA pathogenesis. For instance, WTAP has been shown to promote chondrocyte proliferation and alleviate OA progression (Yang et al. 2025). METTL3 knockdown ameliorates IL-1β-induced chondrocyte injury in OA (Chen et al. 2025). However, the role of another m6A regulator, KIAA1429, in OA progression has not been reported. The current work revealed upregulation of KIAA1429 in IL-1β-treated chondrocytes, a finding corroborated by analysis of the GSE51588 dataset. Functionally, KIAA1429 knockdown enhanced cell viability and suppressed cell death in IL-1β-induced chondrocytes, suggesting a promotive role in OA progression.

Cellular senescence has emerged as a critical feature of OA cartilage, with studies demonstrating that selective elimination of senescent chondrocytes alleviates OA in mice (Liu et al. 2022). Several biomarkers of cellular senescence have been authenticated, including SA-β-gal, p16 and p21 (Huang et al. 2022). Notably, KIAA1429 silencing suppressed these markers, indicating its involvement in promoting chondrocyte senescence. Beyond senescence, ferroptosis – a form of regulated cell death driven by iron overload, ROS accumulation, and GSH depletion – has recently been implicated in OA (Pang et al. 2024; Wu et al. 2024). Iron is an indispensable element for the proper functioning of mammalian cells, and its homeostasis is essential for articular cartilage health (Sun et al. 2021). Excessive iron can lead to oxidative stress injury and ferroptosis of chondrocytes, ultimately triggering the occurrence of OA (Zhang et al. 2025). During this study, data indicated that IL-1β-induced ROS production, Fe^{2+} level increase and GSH reduction were all reversed by KIAA1429 knockdown. As the dominating promoter of ferroptosis, iron-containing enzyme lipoxygenase depends on the activation of ACSL4-related lipid biosynthesis (Chen et al. 2021). On the contrary, the selenium-containing enzyme GPX4 acts as a main inhibitor of ferroptosis and its activity relies on glutathione that is produced through cystine-glutamate antiporter SLC7A11 (Chen et al. 2021). Herein, silencing of KIAA1429 upregulated SLC7A11 and decreased ACSL4 in IL-1β-exposed chondrocytes, suggesting that KIAA1429 contributed to chondrocyte ferroptosis in an OA cell model. This effect of KIAA1429 on chondrocyte ferroptosis is consistent with findings from a previous study (Liu D et al. 2024).

USP3, a key deubiquitinase (DUB) involved in ubiquitination regulation, is aberrantly expressed in a wide range of diseases and plays specific roles in pathological processes (Zhang et al. 2024). Given the predicted m6A binding site in USP3 mRNA, the researchers investigated the potential interaction between KIAA1429 and USP3. KIAA1429 was verified to interact with USP3 and reduce USP3 mRNA stability in an m6A-dependent manner. More importantly, rescue assays suggested that the effects of KIAA1429 knockdown on senescence and ferroptosis were attributed to the upregulation of USP3. Regarding the regulation of USP family members by m6A regulators, METTL3 has been shown to mediate the m6A modification of USP15 in hepatocellular carcinoma (Fang et al. 2025). In this study, KIAA1429 was identified for the first time as a regulator of OA progression *in vitro* by mediating USP3 m6A modification.

The DMM method is commonly used to establish an OA animal model (Wang et al. 2019; Guo et al. 2024). Following DMM induction, significant senescence and ferroptosis were observed, and KIAA1429 knockdown alleviated this damage. Thus, KIAA1429 promotes chondrocyte injury in OA, as demonstrated in both IL-1β-induced chondrocytes *in vitro* and DMM-induced mice *in vivo*. Nevertheless, this study has some limitations. Rescue experiments involving USP3 for KIAA1429 are lacking in DMM-induced mice; therefore, the KIAA1429/USP3 axis will be investigated *in vivo* in future studies. Furthermore, it is unclear whether downstream signals are affected by the KIAA1429/USP3 axis in OA. Given the regulatory role of USP3 as a DUB, exploring its downstream targets may contribute to understanding the molecular mechanism by which the KIAA1429/USP3 axis affects OA.

In conclusion, KIAA1429 reduced USP3 mRNA through m6A modification to promote chondrocyte senescence and ferroptosis in IL-1β-induced OA. The KIAA1429/USP3 was y disclosed for the first time as a regulatory mechanism in OA progression. Targeting KIAA1429 to control senescence and ferroptosis demonstrates potential for the prevention and treatment of OA.

Data availability statement. The datasets are available from the corresponding author on reasonable request.

Authors' contributions. BM is in charge of experimental operation and manuscript drafting. JZ collected the data and constructed the graphs. CC finished the statistical analysis and checked the language and grammar. BY designed the research direction and content.

Conflict of interest. The authors declare that they have no competing interest.

Ethics approval. Ethical approval for the study was acquired from the Animal Care Committee of No. 215 Hospital of Shaanxi Nuclear Industry.

References

Chen C, Chen P, Du Z, Zhang J, Zhou Y (2025): Methyltransferase-like 3-mediated m6A modification of heat shock protein family a member 4-like facilitates interleukin-1beta-induced chondrocyte injury to promote osteoarthritis progression. J Biochem Mol Toxicol **39,** e70492
https://doi.org/10.1002/jbt.70492

Chen X, Li J, Kang R, Klionsky DJ, Tang D (2021): Ferroptosis: machinery and regulation. Autophagy **17,** 2054-2081
https://doi.org/10.1080/15548627.2020.1810918

Coryell PR, Diekman BO, Loeser RF (2021): Mechanisms and therapeutic implications of cellular senescence in osteoarthritis. Nat Rev Rheumatol **17,** 47-57
https://doi.org/10.1038/s41584-020-00533-7

Fang R, Jia Z, Xin Y, Zhao K, Qin W, Lu H, et al. (2025): N6-methyladenosine-modification of USP15 regulates chemotherapy resistance by inhibiting LGALS3 ubiquitin-mediated degradation via AKT/mTOR signaling activation pathway in hepatocellular carcinoma. Cell Death Discov **11,** 3
https://doi.org/10.1038/s41420-024-02282-y

Fujii Y, Liu L, Yagasaki L, Inotsume M, Chiba T, Asahara H (2022): Cartilage homeostasis and osteoarthritis. Int J Mol Sci **23,** 6316
https://doi.org/10.3390/ijms23116316

Glasson SS, Blanchet TJ, Morris EA (2007): The surgical destabilization of the medial meniscus (DMM) model of osteoarthritis in the 129/SvEv mouse. Osteoarthritis Cartilage **15,** 1061-1069
https://doi.org/10.1016/j.joca.2007.03.006

Guo H, Lv Z, Wang M, Li W, Xie Y, Liu Z, Chen F, Jiang R, Liu Y, Wu R, et al. (2024): CD73 alleviates osteoarthritis by maintaining anabolism and suppressing catabolism of chondrocytes extracellular matrix. J Orthop Translat **49,** 96-106
https://doi.org/10.1016/j.jot.2024.08.014

Hongyao X, Yang Z, Zhu P, Zengxin G (2024): Osteoarthritis: Insights into potential causes and biomarkers from articular fluid metabonomics. Curr Proteomics **21,** 293-301
https://doi.org/10.2174/0115701646310314240910082445

Huang W, Hickson LJ, Eirin A, Kirkland JL, Lerman LO (2022): Cellular senescence: the good, the bad and the unknown. Nat Rev Nephrol **18,** 611-627
https://doi.org/10.1038/s41581-022-00601-z

Knights AJ, Redding SJ, Maerz T (2023): Inflammation in osteoarthritis: the latest progress and ongoing challenges. Curr Opin Rheumatol **35,** 128-134
https://doi.org/10.1097/BOR.0000000000000923

Liu D, Ren L, Liu J (2024): METTL14 promotes chondrocyte ferroptosis in osteoarthritis via m6A modification of GPX4. Int J Rheum Dis **27,** e15297
https://doi.org/10.1111/1756-185X.15297

Liu L, Zhang W, Liu T, Tan Y, Chen C, Zhao J, Geng H, Ma C (2023): The physiological metabolite alpha-ketoglutarate ameliorates osteoarthritis by regulating mitophagy and oxidative stress. Redox Biol **62,** 102663
https://doi.org/10.1016/j.redox.2023.102663

Liu Y, Zhang Z, Li T, Xu H, Zhang H (2022): Senescence in osteoarthritis: from mechanism to potential treatment. Arthritis Res Ther **24,** 174
https://doi.org/10.1186/s13075-022-02859-x

Liu Y, Li J, Wang C, Li J, Luo K, Tao K, You J, Wu L, Li W, Jiao Y, et al. (2024a): The m6A writer KIAA1429 regulates photoaging progression via MFAP4-dependent collagen synthesis. BMC Biol **22,** 192
https://doi.org/10.1186/s12915-024-01976-0

Liu Y, Zhang Z, Fang Y, Liu C, Zhang H (2024b): Ferroptosis in osteoarthritis: Current understanding. J Inflamm Res **17,** 8471-8486
https://doi.org/10.2147/JIR.S493001

Mandl LA (2019): Osteoarthritis year in review 2018: clinical. Osteoarthritis Cartilage **27,** 359-364
https://doi.org/10.1016/j.joca.2018.11.001

Pang Q, Tang Z, Luo L (2024): The crosstalk between oncogenic signaling and ferroptosis in cancer. Crit Rev Oncol Hematol **197,** 104349
https://doi.org/10.1016/j.critrevonc.2024.104349

Radbakhsh S, Najar M, Merimi M, Benderdour M, Fernandes JC, Martel-Pelletier J, Pelletier JP, Fahmi H (2025): RNA modifications in osteoarthritis: Epitranscriptomic insights into pathogenesis and therapeutic targets. Int J Mol Sci **26,** 4955
https://doi.org/10.3390/ijms26104955

Ren Q, Chen K, Wang L (2025): Epigallocatechin gallate impels osteogenic differentiation of human BMSCs by targeting the METTL3/SATB2/Wnt/β-catenin axis. Lett Drug Design Discov **22,** 100027
https://doi.org/10.1016/j.lddd.2025.100027

Rim YA, Nam Y, Ju JH (2020): The role of chondrocyte hypertrophy and senescence in osteoarthritis initiation and progression. Int J Mol Sci **21,** 2358
https://doi.org/10.3390/ijms21072358

Sun K, Guo Z, Hou L, Xu J, Du T, Xu T, Guo F (2021): Iron homeostasis in arthropathies: From pathogenesis to therapeutic potential. Ageing Res Rev **72,** 101481
https://doi.org/10.1016/j.arr.2021.101481

Wan Y, Shen K, Yu H, Fan W (2023): Baicalein limits osteoarthritis development by inhibiting chondrocyte ferroptosis. Free Radic Biol Med **196,** 108-120
https://doi.org/10.1016/j.freeradbiomed.2023.01.006

Wang BW, Jiang Y, Yao ZL, Chen PS, Yu B, Wang SN (2019): Aucubin protects chondrocytes against IL-1beta-induced apoptosis

in vitro and inhibits osteoarthritis in mice model. Drug Des Devel Ther **13,** 3529-3538
https://doi.org/10.2147/DDDT.S210220

Wang Y, Shi Y, Niu K, Yang R, Lv Q, Zhang W, Feng K, Zhang Y (2024): Ubiquitin specific peptidase 3: an emerging deubiquitinase that regulates physiology and diseases. Cell Death Discov **10,** 243
https://doi.org/10.1038/s41420-024-02010-6

Wen J, Zhu Q, Liu Y, Gou LT (2024): RNA modifications: emerging players in the regulation of reproduction and development. Acta Biochim Biophys Sin **57,** 33-58
https://doi.org/10.3724/abbs.2024201

Wu F, Zhang L, Lai C, Peng X, Yu S, Zhou C, Zhang B, Zhang W (2022): Dynamic alteration profile and new role of RNA m6A methylation in replicative and H(2)O(2)-induced premature senescence of human embryonic lung fibroblasts. Int J Mol Sci **23,** 9271
https://doi.org/10.3390/ijms23169271

Wu SF, Ga Y, Ma DY, Hou SL, Hui QY, Hao ZH (2024): The role of ferroptosis in environmental pollution-induced male reproductive system toxicity. Environ Pollut **363,** 125118
https://doi.org/10.1016/j.envpol.2024.125118

Yang W, Hu L, Tian Y, Yang Y, Guo W, Xiao K, Yang R, Yang H, Zhou Z, Cheng C (2025): WTAP improves chondrocyte loss and dysfunctions to ameliorate osteoarthritis through mediating the mA methylation and mRNA stability of IL-33. Int J Biol Macromol **306,** 141330
https://doi.org/10.1016/j.ijbiomac.2025.141330

Yao Q, Wu X, Tao C, Gong W, Chen M, Qu M, Zhong Y, He T, Chen S, Xiao G (2023): Osteoarthritis: pathogenic signaling pathways and therapeutic targets. Signal Transduct Target Ther **8,** 56
https://doi.org/10.1038/s41392-023-01330-w

Yu L, Yu G, Wu H, Zhu B, Yin H, Wang W (2025): Curcumin ameliorates the progression of osteoarthritis through the METTL3/OLFM4 pathway. Lett Drug Design Discov **22,** 100148
https://doi.org/10.1016/j.lddd.2025.100148

Zhang H, Liu W, Wu Y, Chen C (2024): USP3: Key deubiquitylation enzyme in human diseases. Cancer Sci **115,** 2094-2106
https://doi.org/10.1111/cas.16178

Zhang X, Li MJ, Xia L, Zhang H (2022): The biological function of m6A methyltransferase KIAA1429 and its role in human disease. PeerJ **10,** e14334
https://doi.org/10.7717/peerj.14334

Zhang Y, Zhang D, Liao X, Xu Q, Bu L, Zheng J, Shen P, Yang C (2025): Novel insights into the role of ferroptosis in temporomandibular joint osteoarthritis and knee osteoarthritis. Int J Med Sci **22,** 2119-2131
https://doi.org/10.7150/ijms.107057

Zhou K, Yuan M, Sun J, Zhang F, Li X, Xiao X, Wu X (2025): Co-delivery of IL-1Ra and SOX9 via AAV inhibits inflammation and promotes cartilage repair in surgically induced osteoarthritis animal models. Gene Ther **32,** 211-222
https://doi.org/10.1038/s41434-025-00515-y

Zhou Q, Xiao Z, Zhou R, Zhou Y, Fu P, Li X, Wu Y, Wu H, Qian Q (2019): Ubiquitin-specific protease 3 targets TRAF6 for deubiquitination and suppresses IL-1beta induced chondrocyte apoptosis. Biochem Biophys Res Commun **514,** 482-489
https://doi.org/10.1016/j.bbrc.2019.04.163

Received: September 26, 2025
Final version accepted: May 5, 2026